Benchmark calculations on residue production within the EURISOL DS project; Part II: Thick targets

J.-C. David, V. Blideanu, A. Boudard, D. Doré, S. Leray, B. Rapp, D. Ridikas, N. Thiollière

CEA Saclay, DSM/DAPNIA, 91191 Gif-sur-Yvette, France
E-mail: jean-christophe.david@cea.fr

1. Introduction

Within the EURISOL-DS [1] project several benchmarks [2, 3, 4] have been done to validate the modelling tools needed to design this new generation RIB (Radioactive Ion Beam) factory. This paper deals with benchmarks on residue production in thick targets using MCNPX2.5.0 [5] and is the third and last one of such series. The first one was dedicated to the particle production on thin and thick targets [2] and the second one to the residue production on thin targets [4].

Very few data exist on residue production with thick targets. Fortunately the only ones which are available coincide with the proton beam energy and target material proposed for EURISOL, namely around 1 GeV for the energy and fissile material (ex.: U) or heavy nuclei (ex.: Pb) for the target. The first set of data, mass distributions of 5 elements, was obtained from ISOLDE [6] ($E_{projectile}$=1.0 and 1.4 GeV; target materials are ThC_x and UC_x). The second set contains the specific activities of 28 radio-nuclides in different places along the thick target, from a dedicated experiment done at Dubna [7] ($E_{projectile}$=660 MeV; target material is natural Pb).

Comparisons between calculations and data have been performed and lead to quantitative conclusions on the capabilities of the different spallation models within MCNPX concerning the residue production in thick targets.

2. ISOLDE data

At the PBS-ISOLDE facility (CERN) yields of noble gas isotopes were measured [6] from UC_x and ThC_x targets, and in this way Ne, Ar, Kr, and Xe in-target mass distributions were determined. With the ISOL (Isotope Separation On-Line) method nuclei are produced in the target, they diffuse and are ionized to provide the secondary radioactive beam. Then, delay time due to diffusion out of the target and ionization efficiency had to be previously determined to get the in-target yields from the activities obtained experimentally. Details of the method can be read in the reference [6].

Data for five isotopes are available from the UC_x target impinged by a 1.4 GeV proton beam (Gaussian shape, $\sigma_x=\sigma_y=0.7$ cm), namely Xe, Kr, Ne, Ar and Zn, and data for two isotopes from the ThC_x target impinged by a 1.0 GeV proton beam (same shape), namely Xe and Kr. Targets (L=20 cm; Φ=1.8 cm) were enclosed in graphite cylinder of d=0.2 cm thickness and then in a Ta cylinder (d=0.2 cm).

Calculations were performed using the transport code MCNPX2.5.0 [5] taking into account exact geometry of the targets and also the time-dependent decays (cumulative yields $\equiv$ individual yields of the element including its parents). Three model combinations were studied: INCL4[8]-Abla[9], Isabel[10]-Abla and CEM2k[11]. A previous study on thin targets [4] showed they were the most suitable ones to reproduce residue yields.

2.1 p(1.4GeV) + UC$_x$

Light nuclei: Ne and Ar (see Fig.1)

No model reproduces these data. INCL4-Abla and Isabel-Abla give almost no yields for Ne. In the case of Ar, if the shape seems quite good, the rate is too low. CEM2k gives sometimes the right rate, but only for very few isotopes; indeed, the shape of mass distributions is too broad as already observed in the case of thin targets.

We add separately that improvements of INCL4 and Abla are in progress and could solve the underlined discrepancies in the near future. Equally, CEM03, new release of CEM2k, can already be run with a beta version of MCNPX. Therefore, one expects these new predictions obtained with the last official version of MCNPX, MCNPX2.5.0, to become more reliable in the coming years.
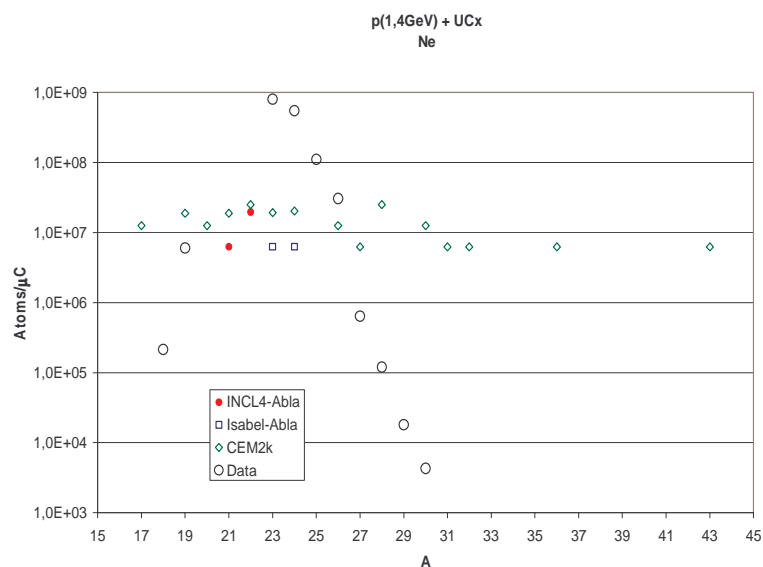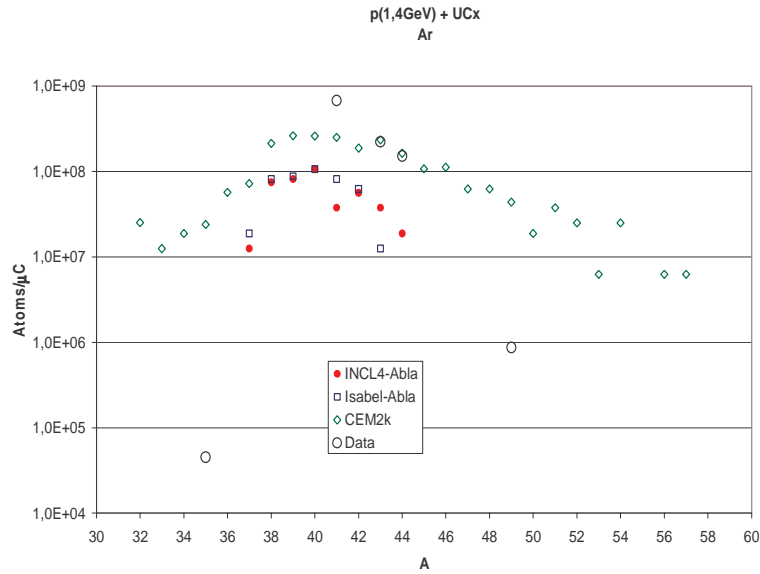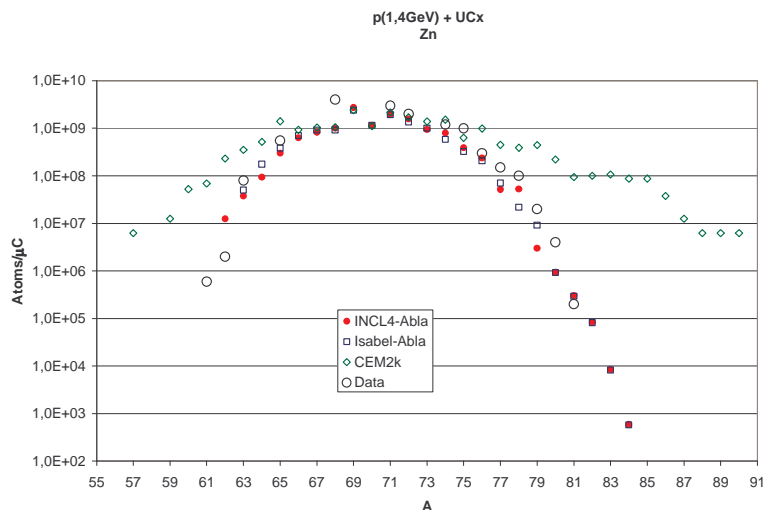
Figure 1: *Mass distributions of Ne (top) and Ar (bottom) obtained with UC$_x$ thick target impinged by 1.4 GeV proton beam. Data (black open circle) are from ISOLDE [6] and calculations were made with MCNPX2.5.0. Three different model combinations were examined: INCL4-Abla (red full circle), Isabel-Abla (blue open square) and CEM2k (green open diamond).*

<u>Fission products</u>: Zn, Kr and Xe (see Fig. 2)

INCL4-Abla and Isabel-Abla have not only the right shape but also give reasonable absolute production rates; in most of the cases the experimental yields are reproduced within a factor of 2 (Kr and Xe) or 3 (Zn). In some cases even better agreement is reached. CEM2k again gives two broad distributions and might be "wrong" by a few orders of magnitude on the neutron rich or neutron deficient sides (see Fig. 2).
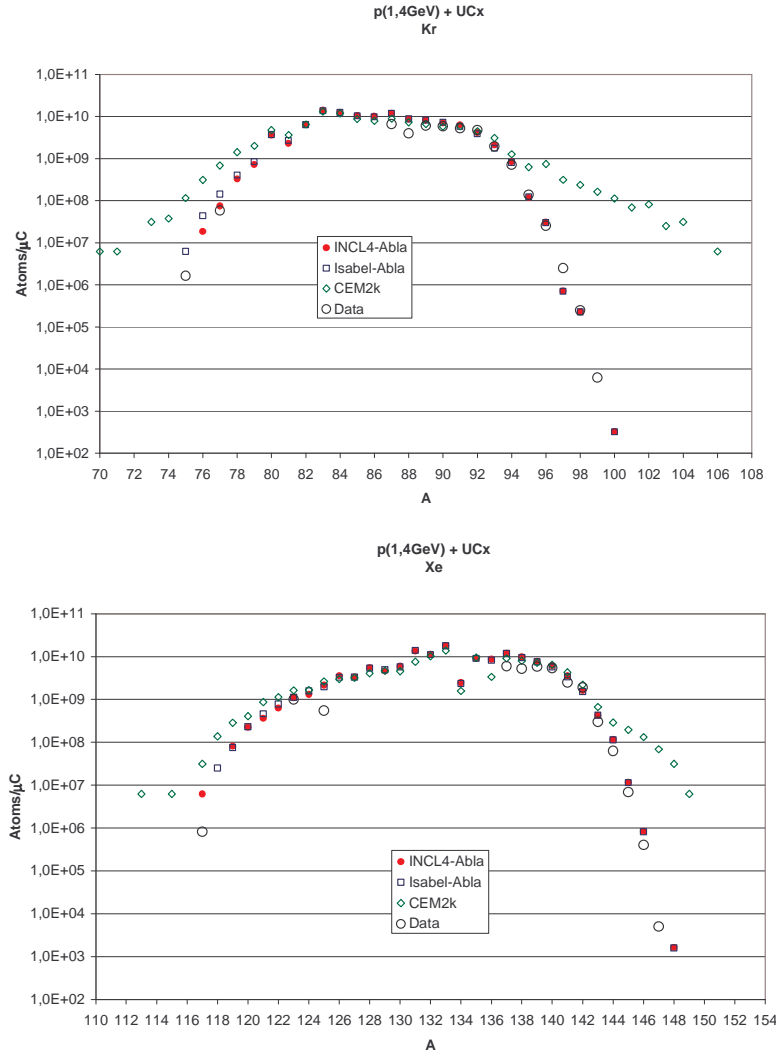
Figure 2: *Mass distributions of Zn (top), Kr (middle) and Xe (bottom) obtained with UC$_x$ thick target impinged by 1.4 GeV proton beam. Data (black open circles) are from ISOLDE [6] and calculations were made with MCNPX2.5.0. Three different model combinations were examined: INCL4-Abla (red full circle), Isabel-Abla (blue open square) and CEM2k (green open diamond).*

Contributions from different reaction channels (see Fig. 3)

In this work we studied for each group of nuclei the importance of 1) the contributions of the parent nuclei through their decay (cumulative yields compared to individual yields) and, 2) the contribution from the reactions induced by the secondary neutrons below 20 MeV. We remind in this context that the residues from high energy projectiles are taken into account directly by MCNPX, but residues from low energy neutrons were obtained using some fission yield tables [12] combined to the low energy neutron-induced fission rates. We detail below the results for Ar (light nucleus) and Kr (fission product).
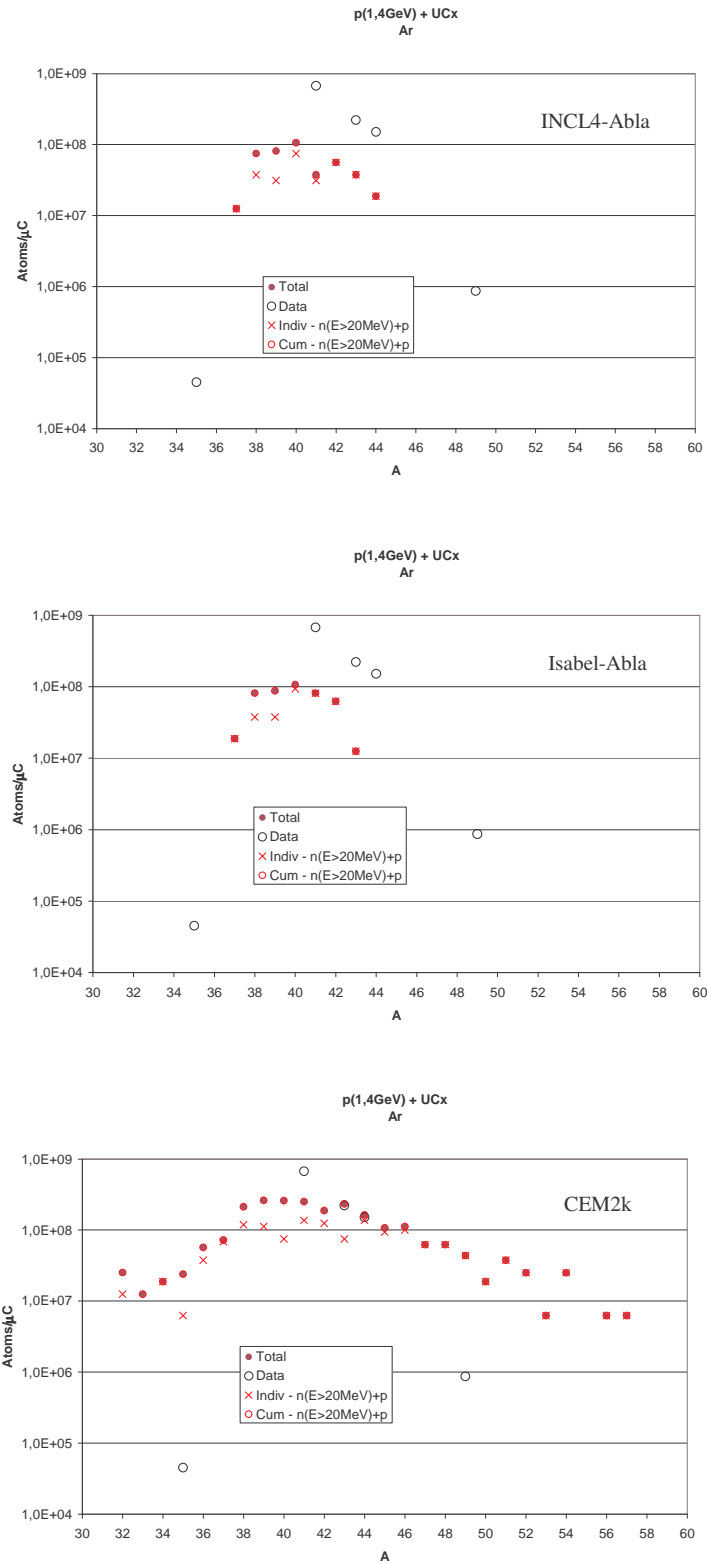
Figure 3a: *Contributions of the parent nuclei decay to the yields for Ar, produced with the UC$_x$ thick target impinged by 1.4 GeV proton beam. Data (black open circles) are from ISOLDE [6] and calculations were made with MCNPX2.5.0. Results of three spallation models are shown from top to the bottom respectively: INCL4-Abla, Isabel-Abla and CEM2k. Total = cumulative from n(E>20MeV) and light charged particles + cumulative from n(E<20MeV).*
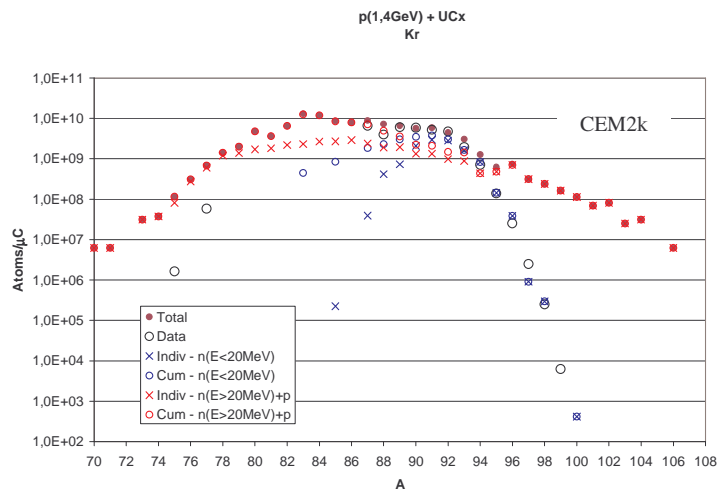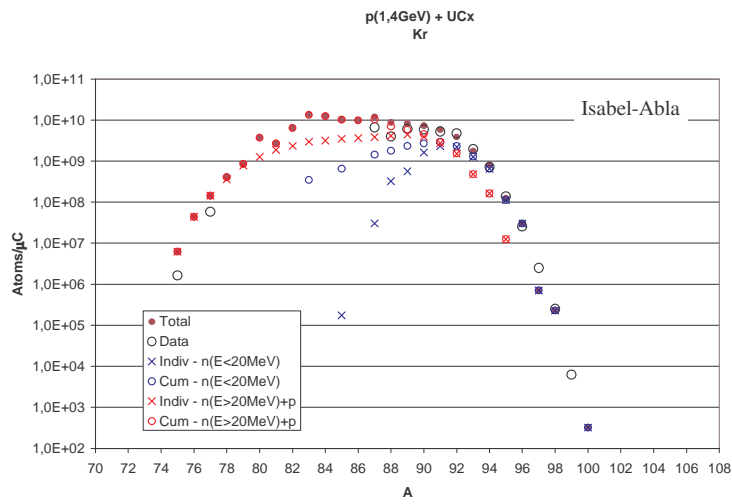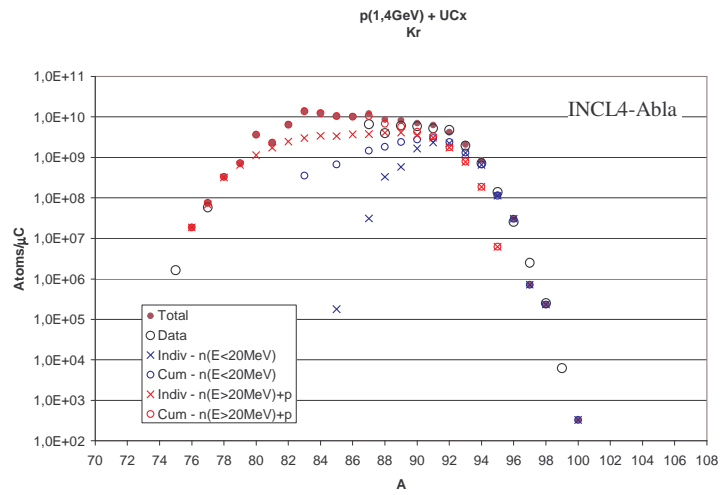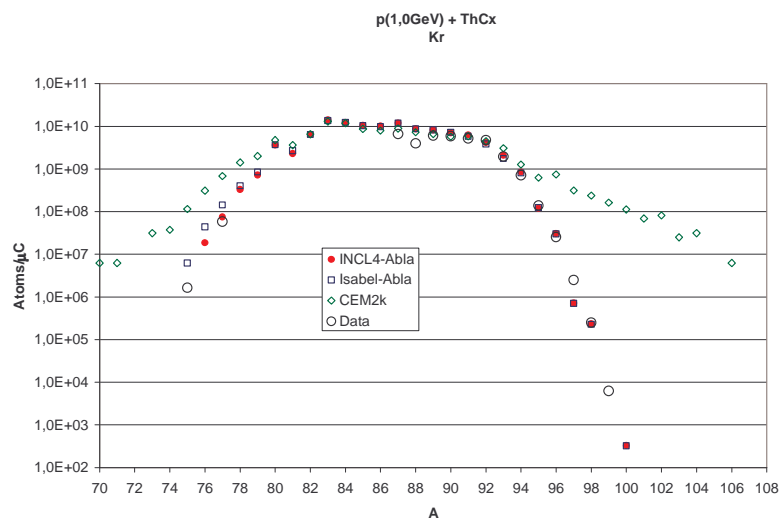
Figure 3b: *Contributions of the parent nuclei decay and of the low energy neutrons to the yields for Kr, produced with an UC$_x$ thick target impinged by 1.4 GeV proton beam. For details see Figs. 3a.*

First of all, one can see that cumulative yields (open circles) are different from individual ones (crosses) for isotopes close to the stable ones (e.g., around A=39 for Ar, and around A=85 for Kr), and this difference can not be neglected whatever the nucleus studied.

Low energy neutrons, as expected, play an important role only for the fission products since high energy particles are necessary to produce light residues due to different reaction mechanism. These low energy neutrons are responsible mainly for the neutron rich side of the mass distributions using the INCL4-Abla and Isabel-Abla models, but not for CEM2k. One can clearly understand that CEM2k in this region is wrong because of its overestimation of neutron rich (and also neutron deficient) isotopes by the high energy particles.

2.2 p(1.0GeV) + ThC$_x$

In this case data exist only for Kr and Xe isotopes. The conclusions are the same as the ones already reported for UC$_x$. The only significant difference is a "*bump*" around the mass A=140 in the case of Xe (see Fig. 4), and this increase is not reproduced by our three spallation models. This *bump* is located around the low energy neutron contribution peak as seen from Fig. 5, what makes our analysis even more difficult: It is not clear whether low energy neutron data tables or high energy spallation models fail. At the same time, more data on ThC$_x$ would be very much helpful.
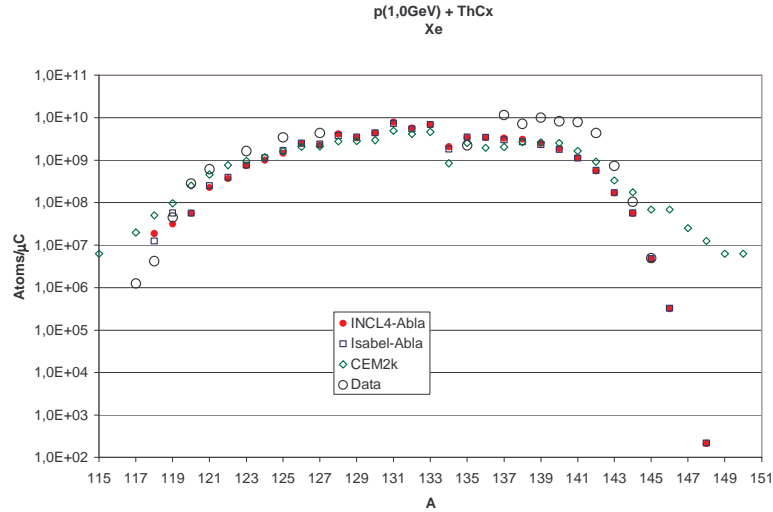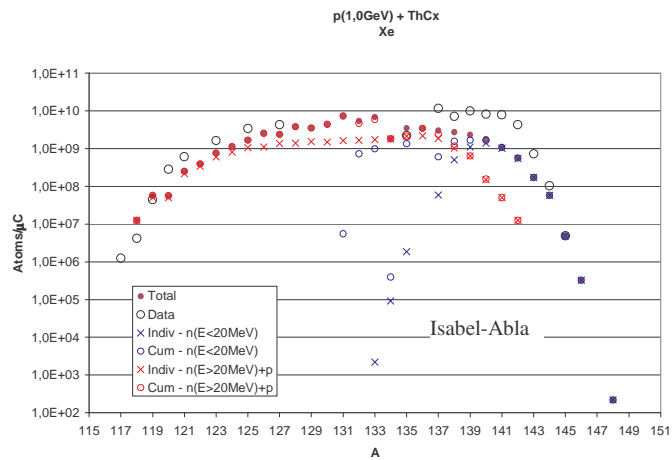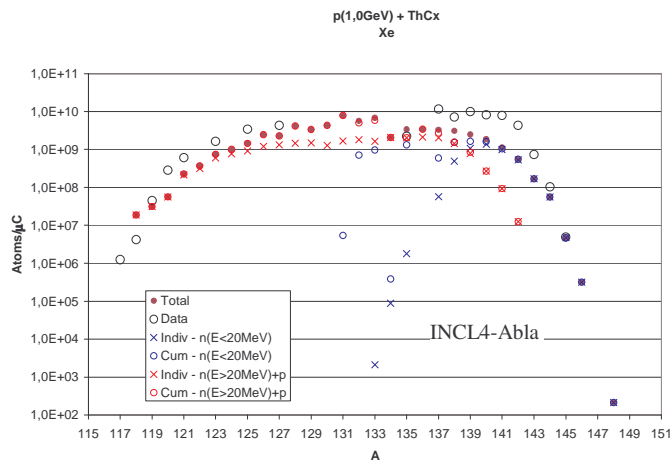
Figure 4: Mass distributions of Kr (left side) and Xe (right side) obtained from a ThC_x thick target impinged by 1.0 GeV proton beam. Data (black open circles) are from ISOLDE [6] and calculations were made with MCNPX2.5.0. Three spallation models were used: INCL4-Abla (red full circles), Isabel-Abla (blue open squares) and CEM2k (green open diamonds).
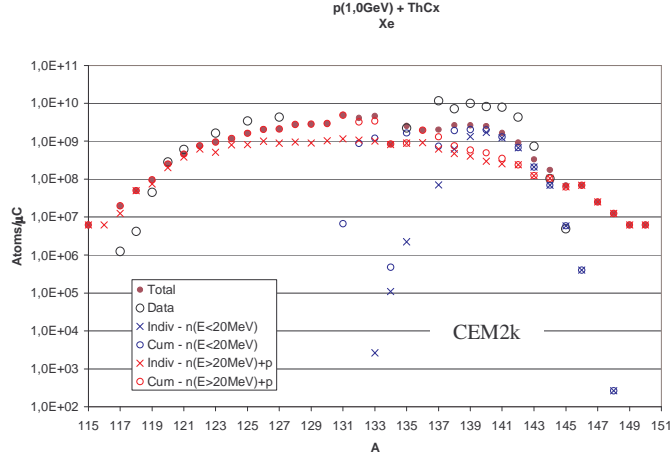
Figure 5: *Contributions of the parent nuclei decay and of the low energy neutrons to the yields of Xe produced with a ThC$_x$ thick target impinged by 1.0 GeV proton beam. Data (black open circles) are from ISOLDE [6] and calculations were made with MCNPX2.5.0. Results of three spallation models are shown: INCL4-Abla (on the left), Isabel-Abla (on the right) and CEM2k (on the bottom).*

3   Dubna experiment

It is important to stress that the knowledge of the residue production in thick spallation targets remains very poor. Contrary, in the case of thin targets the experimental excitation functions of residue production cross sections do exist [13] and gives us the opportunity to test the models on a wide projectile energy range, mainly for protons. Of course, we have no experimental information about the particle spectra in the case of thick targets.

The previously described ISOLDE data are therefore very interesting, but they are integrated on the whole target and they do not come from a dedicated experiment, so only few elements are considered (this is also related to the well controlled extraction efficiencies for rare gases). Fortunately, data obtained recently on a thick lead target in Dubna by Krakow-Moscow collaboration are the first ones which are particularly suited to benchmark codes on residue production in a thick target including the dependence on the geometrical position along the target [7].

In this experiment the target was a natural lead cylinder (L=30.8 cm; Φ=8.0 cm) made of several bulky pieces including 31 foils (1.0 mm thick) used as irradiation samples. The 660 MeV proton beam fluence, $26.3 \pm 1.9 \times 10^{13}$ protons, were obtained with an irradiation time of 9 h. Intensity and beam distribution was monitored thanks to an ionization chamber and Al foils. As a result of this experiment, distributions of the specific activities of 28 radionuclides along the lead target were measured and analysed.

Corresponding calculations performed to compare the specific activities measured at Dubna in this thick lead target were done with MCNPX2.5.0 followed by the evolution code CINDER'90 [14]. The exact geometry as used during the experiment was modelled. Bertini[15]-Dresner[16], INCL4-Abla, Isabel-Abla and CEM2k are the spallation models we used in MCNPX. For each model we run 20 millions events, which represent several days of

computer time. In some cases we will see that more statistics would be necessary to draw more precise conclusions.

3.1 Models compared to data

Figures 6 to 12 present some typical results we obtained. These include: A light or intermediate mass nucleus (^{59}Fe – Fig. 6); two fission fragments, one on the neutron deficient side (^{88}Y – Fig. 7) and the other one rather on the neutron rich side (^{95}Nb – Fig. 8); two nuclei produced after the evaporation stage, one far from the target nucleus (^{172}Lu – Fig. 9) and the other one closer to the target nucleus (^{183}Re – Fig. 10); and finally a nucleus with a mass very close to the target nucleus (^{207}Bi – Fig. 11 and 12).

Concerning ^{59}Fe (Fig. 6), although we run 20 millions events, too few nuclei are produced by the models (activities are low) and so, if the results are not so bad, at this stage no conclusion among the models can be drawn since the calculation/data ratios are too irregular. For this reason in some figures we added "a yellow shadow" to specify the region where the number of nuclei responsible of the specific activity for the studied nucleus (and its parent) is lower than ~100 atoms.

Neutron rich fission fragments (Fig. 8) are well reproduced by INCL4-Abla and Isabel-Abla whereas CEM2k and Bertini-Dresner underestimate them. This is also true in the case of Bertini-Dresner for the neutron deficient fission fragments (Fig. 7), but does not apply for the predictions obtained by CEM2k. If now Isabel-Abla gives again reasonable results, INCL4-Abla has a production rate somewhat too low, but both models are within a factor of ~2.

Isabel-Abla is also a reliable model to reproduce the nuclei obtained after evaporation. If INCL4-Abla is very good also when the evaporation step is short (Fig. 10), the quality decreases when the evaporation process becomes longer and longer, i.e. more and more particles are evaporated (Fig. 9). Contrary, Bertini-Dresner always overestimates the data, while CEM2k becomes a good model candidate. In brief, the predictions are within a factor of ~2-3.

For ^{207}Bi (Fig. 11) the results depend strongly which region is considered: Before the Bragg's peak or around the Bragg's peak itself (Fig. 12). All models give very good results before the peak, especially INCL4-Abla and Isabel-Abla, but around the peak the situation is not clear. It seems that these two models could give much better results than CEM2k and Bertini-Dresner, unless this peak were 5 mm beyond the one as expected by the data. It is interesting to note that simply a slight increase in averaged density of the target would bring the model calculations in nearly perfect agreement with data.

Figs. 13a and 13b summarize the calculation/data ratios for the nuclei, where the Monte Carlo statistics is acceptable. Isabel-Abla is the best model giving the predictions compared to data within a factor of ~2. INCL4-Abla gives almost the same results except for the nuclei far from the target and obtained by the evaporation process (within a factor of ~3). If Bertini-Dresner overestimates all fission products (by a factor of 3 and even more), CEM2k is better for the neutron poor fission fragments (similar results as INCL4-Abla) than for the neutron rich ones (within a factor of 4). In the case of other nuclei Bertini-Dresner and CEM2k stay within a factor of ~2.
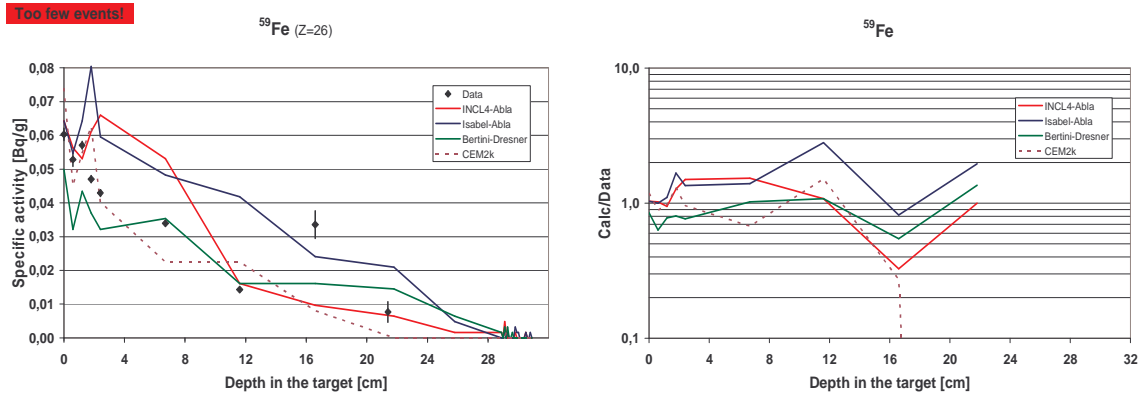
Figure 6: *Specific activities of a light nucleus (^{59}Fe) inside a Lead target. Four spallation models within MCNPX2.5.0 (INCL4-Abla, Isabel-Abla, Bertini-Dresner and CEM2k) are compared to data [7] on the left side and calculation/data ratios are plotted on the right side.*
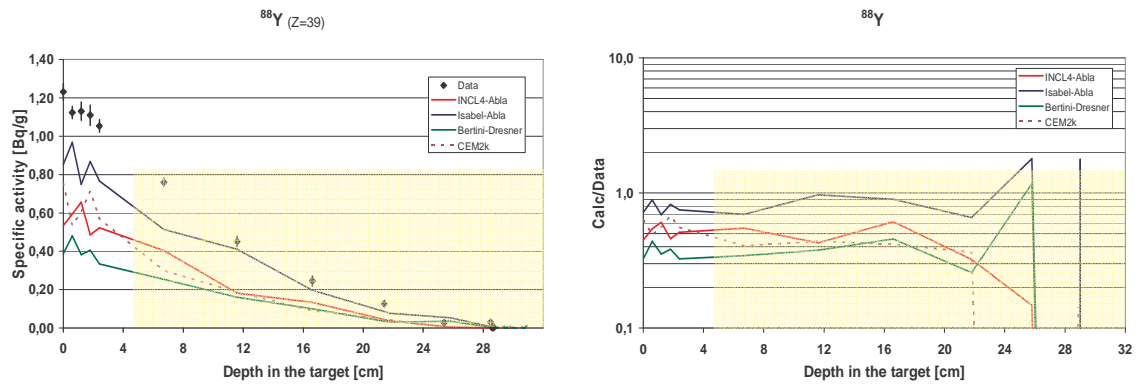

Figure 7: *Specific activities of a neutron deficient fission fragment (^{88}Y). Yellow shadow points out the place where we obtained rather poor statistics (see Fig. 6 for further details).*
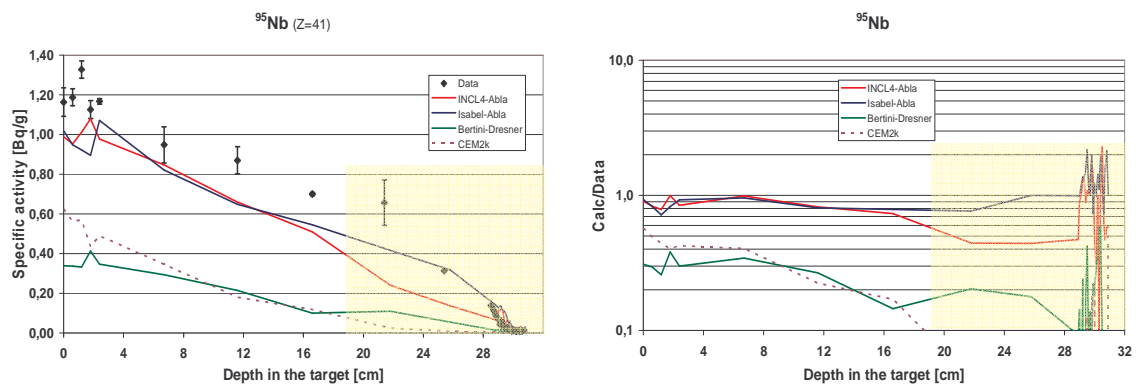

Figure 8: *Specific activities of a neutron rich fission fragment (^{95}Nb). For details see Figs. 6 and 7.*
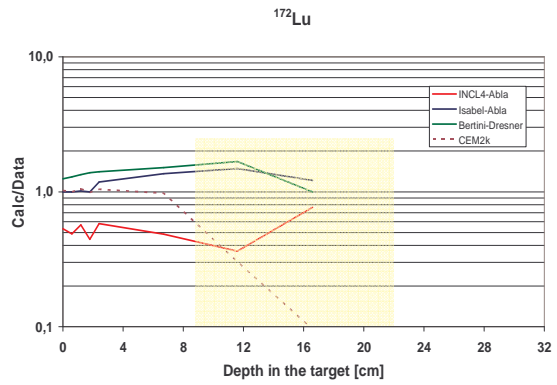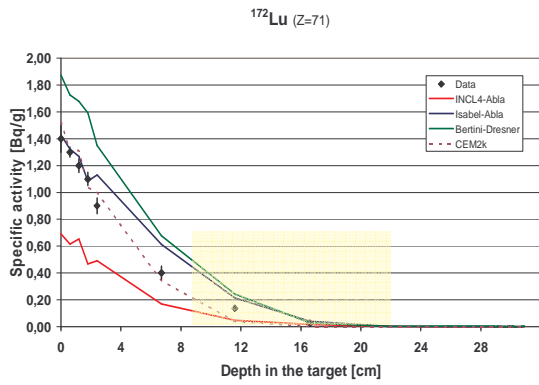
11

Figure 9: *Specific activities of an evaporation residue far from the target (^{172}Lu). For details see Figs. 6 and 7.*
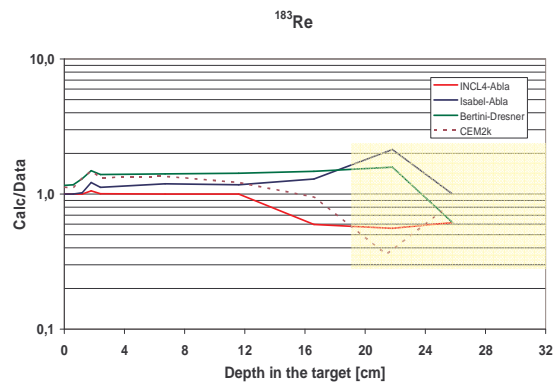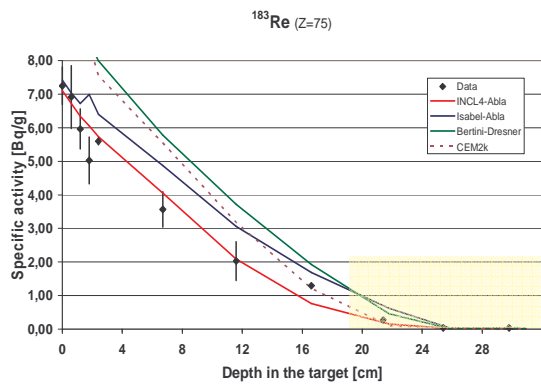

Figure 10: *Specific activities of a nucleus produced after evaporation (^{183}Re). For details see Figs. 6 and 7.*
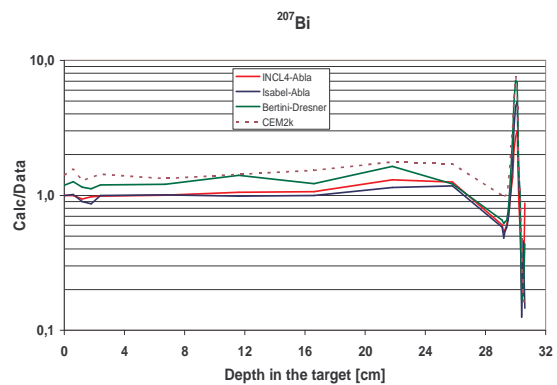

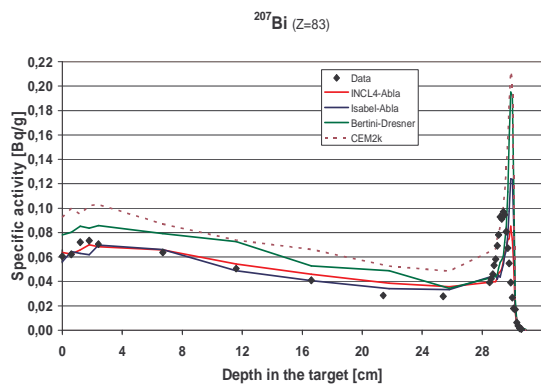**Figure 11:** *Specific activities of a nucleus close to the target (^{207}Bi). For details see Figs. 6 and 7.*
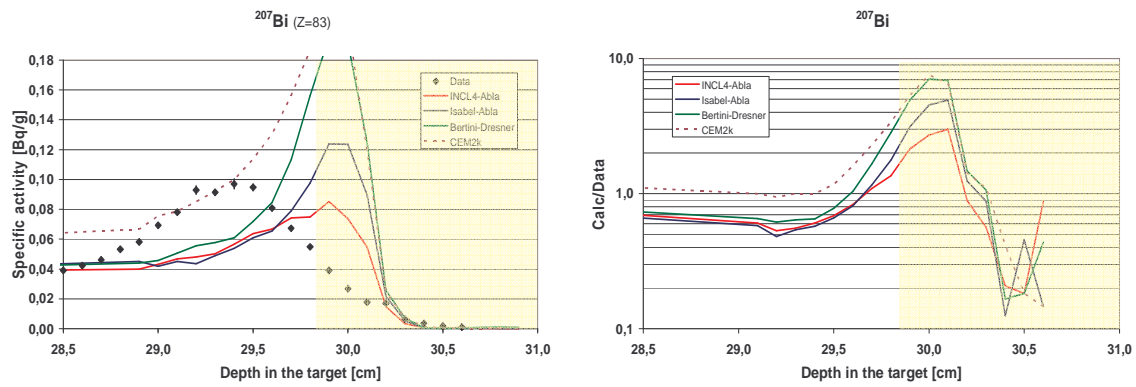
Figure 12: *Same as Fig. 11, but zoomed on the region around the Bragg's peak.*
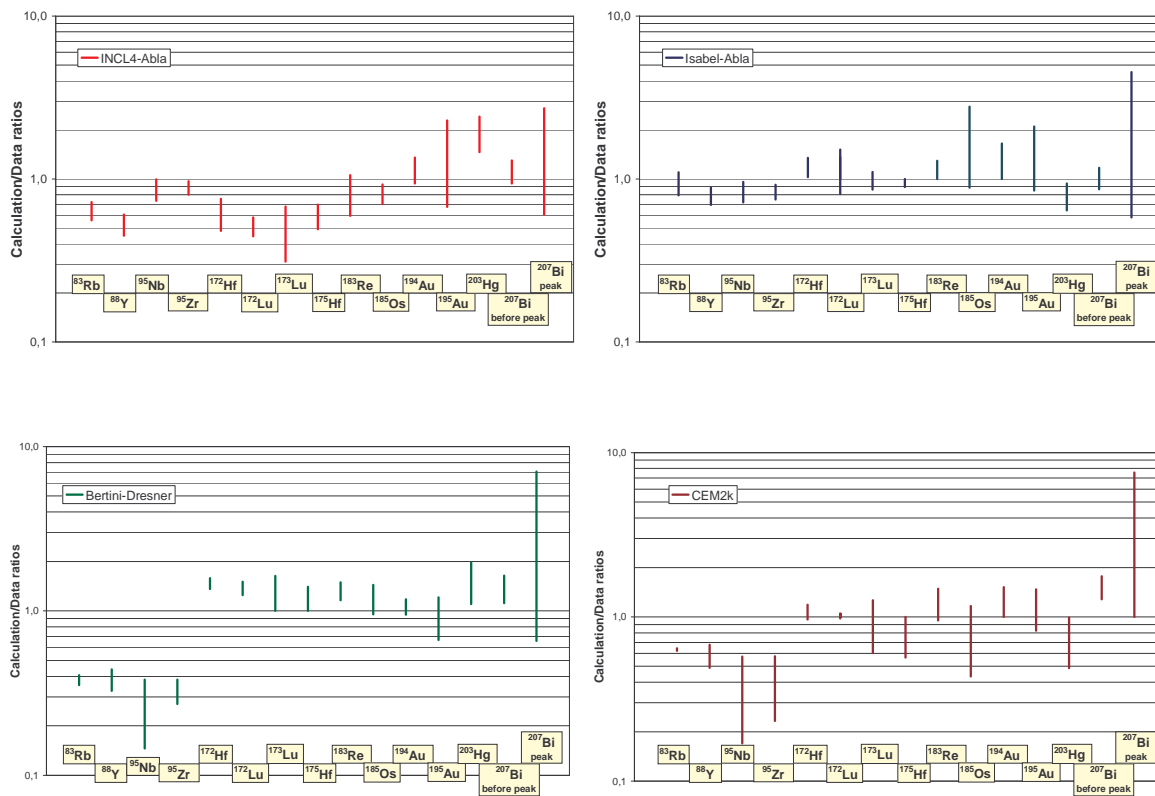

Figure 13a: *Calculation/data ratios in the whole target for the nuclei with the statistics obtained by the models providing more than ~100 atoms. For each isotope (mass increasing from the left (^{83}Rb) to the right (^{207}Bi)) the line gives all possible values for the ratio. Models shown are INCL4-Abla, Isabel-Abla, Bertini-Dresner and CEM2k*
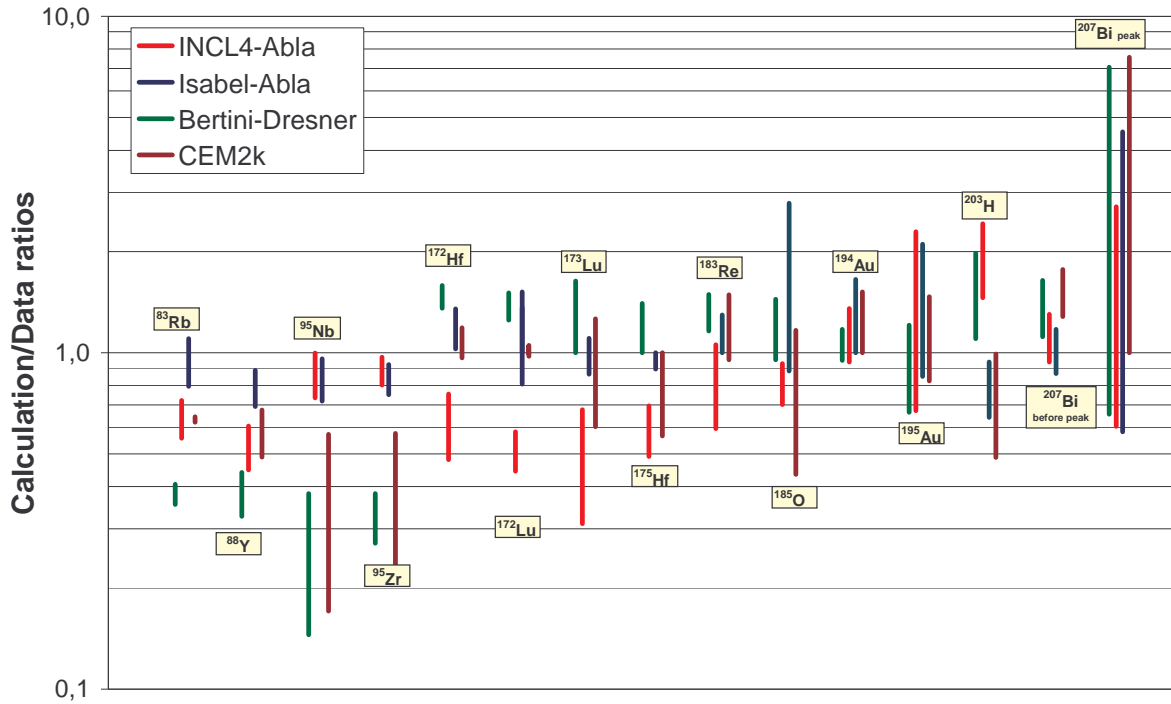
Figure 13b: Summary of Fig. 13a

3.2 Contributions of the primary and secondary particles

Radioactive nuclei are produced in the lead target via the primary protons, i.e. the beam particles, eventually slowed down, and via the secondary particles, that are essentially protons and neutrons, originating from the same spallation reactions. In Figs. from 14 to 16 we studied the weight of each type of particle in the nucleus production inside the target. If all nuclei are produced principally by the primary protons everywhere in the target (along the target axis, since activities are integrated over the radius), the different contributions depend strongly of the studied nucleus and might change with the production position inside the target. Of course, no nuclei are produced by primary protons at the very back of the target since no primary protons reach this position.

In Fig. 14 the case on the production of a fission product, ^{95}Zr, is plotted. Secondary protons and neutrons contribute with a level around 10 % each. The contribution from protons is however a little bit higher than from neutrons, except at the very end of the target, since the latter ones penetrate easier and are less slowed down. This higher contribution by protons can be probably explained by the fissility parameter. This quality of "being fissile" depends on the ratio Z^2/A of the fissioning nucleus and in the mass region of lead, higher Z^2/A is, higher the probability to fission will be. So, for a given target, the parameter Z^2/A is greater with a proton projectile ($Z=Z_{target}+1$) than with a neutron ($Z=Z_{target}$). Indeed, this is also confirmed by Prokofiev's systematics based on some existing data from p+Pb,Bi and n+Pb,Bi.

For the ^{203}Hg isotope (Fig. 15), primary proton contribution is only ~65 % (more at the front, ~80 %, and less at the back of the target, ~40 %). If secondary proton role is about 5 %, neutron importance is around 35 %. The difference between these two secondary particle

types for ^{203}Hg is the following. To get ^{203}Hg via p+^{208}Pb (n+^{208}Pb), 3(2) protons and 3(4) neutrons have to be emitted (see equations below).

$$p + {}^{208}Pb \rightarrow {}^{203}Hg + 3p + 3n$$
$$n + {}^{208}Pb \rightarrow {}^{203}Hg + 2p + 4n$$
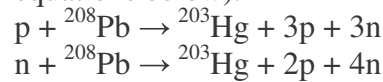
Only the secondary particles coming from the Intra-Nuclear Cascade (INC) stage are able to induce such a reaction. During this process neutrons and protons are ejected with the same probability and then the neutron/proton (emitted) ratio is equal to the N/Z ratio of the nucleus undergoing the reaction. This infers that, for a ^{208}Pb target (N/Z=~1.5), if 3(2) protons are emitted ~4.5(3) neutrons get out also during INC, keeping in mind that other neutrons (and very few protons) can be emitted by evaporation. Then it becomes obvious that secondary neutrons have more chance to produce ^{203}Hg from ^{208}Pb than secondary protons. One can probably explain in the same manner the fact that secondary neutron contribution at the back of the target is higher than the one from primary protons, since the flux (and their energy) of the latter ones decreases in such a way it can no more balance the *most natural* way to create ^{203}Hg from ^{208}Pb.

The situation is completely different for ^{207}Bi (Fig. 16), since bismuth can not be produced via n+Pb. Proton is the only way to produce Bi and, since low energy projectiles are able to create ^{207}Bi from ^{208}Pb (very few particles must be emitted), the contribution from secondary protons is quite high: ~20 % and even more. Obviously the slow down affects more the secondary (low energy) protons than the primary (high energy) protons, that is the reason why secondary proton contribution fall down quickly inside the target.

No significant differences between the models appear concerning the contributions from primary protons (beam), secondary protons and neutrons. This is principally due to the main contribution of the primary protons, so only their transport play a role. Nevertheless, the slight differences seen between the three models perhaps would be more pronounced with a radial distribution, where the proton beam itself is much less important. Such measurements are desired in the future.
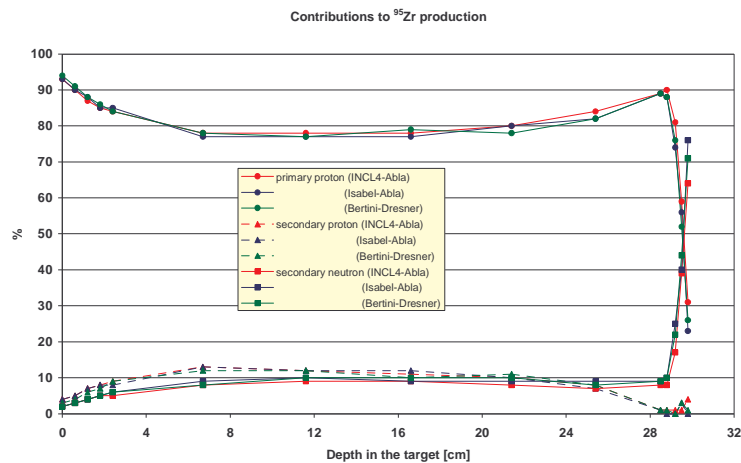

Figure 14: Contributions of the primary protons (beam) and the secondary protons and neutrons (from spallation reactions) to the production of ^{95}Zr. INCL4-Abla, Isabel-Abla and Bertini-Dresner are used here as possible model combinations.

Figure 15: *Contributions of the primary protons (beam) and the secondary protons and neutrons (from spallation reactions) to the production of ^{203}Hg. INCL4-Abla, Isabel-Abla and Bertini-Dresner are used here as possible model combinations.*
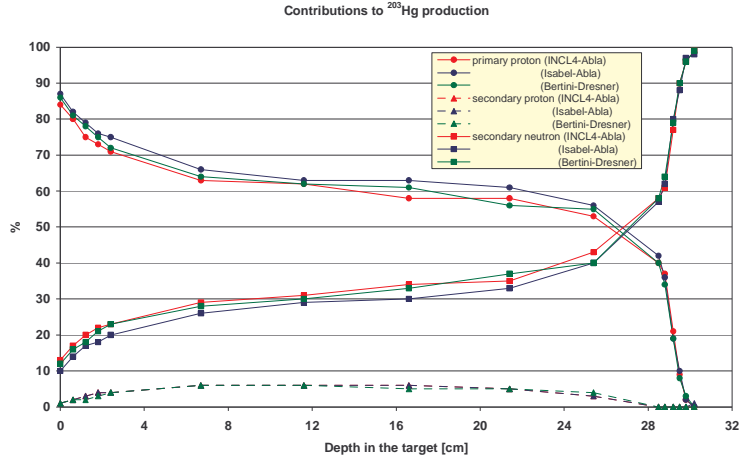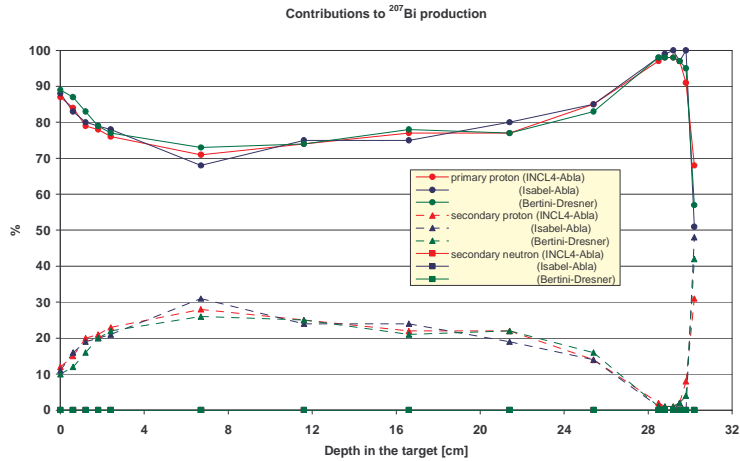

Figure 16: *Contributions of the primary protons (beam) and the secondary protons and neutrons (from spallation reactions) to the production of ^{207}Bi. INCL4-Abla, Isabel-Abla and Bertini-Dresner are used here as possible model combinations.*

4   Conclusion

In this work we benchmarked the predictive capabilities of MCNPX2.5.0 on residue production in thick targets as U, Th and Pb thanks to two sets of data, from ISOLDE [6] and from Dubna [7]. The following conclusions are drawn:

- No model within MCNPX gives reasonable results for the light nuclei with masses lower than "usual" fission products, say, A<50.
- Isabel-Abla seems to give the best results, often similar with INCL4-Abla, which would be less precise in the case of nuclei obtained by the evaporation process, and far from the target nucleus.
- CEM2k gives quite good results, except for the fission products, especially on the neutron rich side.
- Bertini-Dresner, which is the default option in MCNPX2.5.0, is almost always less good than the other three options.

Quantitatively the MCNPX predictions are often within a factor of 2 for the best models, and might be even better when the Isabel-Abla combination is used, what we recommend at the time being. Improvements are in progress for INCL4 and Abla. In addition, a new version of CEM2k, called CEM03, already exists for beta testers of the code, and should be benchmarked in the near future. Therefore, one expects that the model predictions will improve further. In any case, the theoretical efforts should be accompanied by the new dedicated experimental programs.

Taking into account the above conclusions including the benchmarks on residue production from thin targets [4] and on particle production [2] both from thin and thick targets, **the use of Isabel-Abla or INCL4-Abla within MCNPX 2.5.0 is recommended.**

5 Acknowledgement

References

[1]   More information at http://www.eurisol.org

[2]   B. Rapp et al., "Benchmark calculations on particle production within the EURISOL DS project", CEA Saclay , Mar. 2006   ---   http://www.eurisol.org/ (TN-06-04)

[3]   M. Felcini et al., "Validation of FLUKA calculated cross-sections for radioisotope production in proton-on-target collisions at proton energies around 1 GeV", CERN, Jan. 2006   ---   http://www.eurisol.org/ (TN-06-01)

[4]   J.-C. David et al., "Benchmark calculations on residue production within the EURISOL DS project; Part I: thin targets", CEA Saclay Internal report: DAPNIA-07-04; available at http://www.eurisol.org/

[5]   MCNPX User's Manual, Version 2.5.0, April, 2005, LA-CP-05-0369, Denise B. Pelowitz, editor

[6]   CERN-EP/2002-048

[7]   W. Pohorecki *et al*, NIMA 5362 (2006) 750-754, and private communication

[8]   A. Boudard *et al.*, Phys. Rev. C, 66 (2002) 044615)

[9]   A. R. Junghans *et al.*, Nucl. Phys. A 629 (1998) 655

[10]   Y. Yariv and Z. Fraenkel, Phys. Rev. C, 20 (1979) 2227; Y. Yariv and Z. Fraenkel, Phys. Rev. C, 24 (1981) 488)

[11]   S. G. Mashnik and A. J. Sierk, "Recent Developments of the Cascade-Exciton Model of Nuclear Reactions," Los Alamos National Laboratory Report LA-UR-01-5390, Los Alamos (2001)

[12]   Data tables available from: http://ie.lbl.gov/fission.html

[13]   M. Gloris *et al.,* Nucl. Instr. and Meth. A 463 (2001) 593-633

[14]   W.B. Wilson and T.R. England, "A Manual for CINDER'90 Version C00D and Associated Codes and Data", LA-UR-00-Draft, April 2001.

[15]   H.W. Bertini, Phys. Rev. 131, (1963) 1801; H.W. Bertini, Phys. Rev. 188, (1969) 1711).

[16]   L. W. Dresner, ORNL-TM-196 (1962)